

AN EXPERIMENTAL INVESTIGATION OF A PLUNGING WING UNDER GUST ENVIRONMENT

Ilgin KAL¹, Berk ZALOĞLU², Idil FENERCİOĞLU³, Okşan ÇETİNER⁴
Istanbul Technical University
Istanbul, Turkey

ABSTRACT

The performance of a sinusoidally plunging wing under three different gust types is investigated in a water channel. Four gust encounter times are considered to examine the effect of gust on the wing plunging at four different frequencies. Direct force/moment measurements in conjunction with simultaneous DPIV measurements are acquired in order to determine the performance of the plunging wing under vortex gust and to visualize corresponding flow structure interactions.

INTRODUCTION

Air industry have recently directed their interest towards unmanned air vehicles due to their functions in both defense and search/rescue areas. Including the fixed winged unmanned air vehicles, the size of these vehicles are small as compared to commercial aircrafts and the cruise velocity is very low as compared to fighter jets. Hence, the atmospheric fluctuations that the unmanned air vehicles are subject to, might reach critical rates resulting in control difficulty of such vehicles which are expected to be highly agile (Viswanath and Tafti [2010]; Watkins et al. [2006]). Considering the aerodynamics and flight performances, the capability of maneuvering and maintaining steady flight conditions in an unsteady environment is of great importance to the design of unmanned air vehicles. The literature on unmanned air vehicles mostly consists of investigations on simplified models of unsteady flows such as the flow structures around hovering models and vehicles in forward flight. Nevertheless, unmanned air vehicles are expected to be capable to have controlled flight even under unsteady flow conditions such as gusts that match their own forward flight speeds and scales. In recent years, the flow control under gusts in general are getting increased interest (Jones and OI [2014a]; Irving and Smith [2013]). However, the effects of gust on the flow structures around an airfoil and on the unsteady aerodynamic forces and moments are not yet readily known (Jones and OI [2014b]). Other than the unmanned air vehicles, the gust effect also draws attention for helicopter blades, flapping wing micro-air vehicles (MAVs) and wind turbines due to the

¹ Undergraduate student in Astronautical Engineering Department, Email: kali@itu.edu.tr

² Graduate student in Aeronautical and Astronautical Engineering Department, Email: zaloglu@itu.edu.tr

³ Post Doc Researcher/Lecturer in Astronautical Engineering Department, Email: fenercio@itu.edu.tr

⁴ Professor in Astronautical Engineering Department, Email: cetiner@itu.edu.tr

unsteady flow conditions of their working environment and/or their motion. Those small air vehicles and aforementioned systems need to correct their positions and directions when encountered with high altitude winds and gust. Although it is relatively easier to numerically create and control the gust effect, the complex flow structures of unmanned air vehicles during their cruise conditions and maneuvering result in difficulty solving the vortex dynamics around and in the wake of the airfoils. Thus, the numerical studies require extensive experimental data validation. And for experimental investigations, new approaches are required to study the gust effect in detail on the aerodynamic performance and control of micro air vehicles, since it is experimentally difficult to create controlled and uniform gust.

Atmospheric gust modelling and turbulence studies were initiated by NACA in 1915 (Murrow et al. [1989]). The first analytical models used were ondiscrete gusts that caused a change in the instantaneous and one-time constant value at the free-flow velocity (Roadman and Mohsen [2009]) and the gust was shown as a constant term added in streamwise or transverse direction.

Recent experiments were carried out by placing two consecutive wings in the experimental setup and creating gust on the rear wing by oscillating/flapping the fore wing (Neumann and Mai [2013]; Shao et al. [2010]), the studies focused on the applications of fixed wings and performed in wind tunnels. Although there is interest to investigate the gust effect recently, the formation and characterization of spanwise gust remains almost unstudied.

The aim of this study is to carry out simultaneous force/moment measurements with quantitative flow visualization for a plunging airfoil in order to put forward the effect and control of vortical gusts on the design and performance of flapping micro-air vehicles. In this context, three different gust types and four gust encounter times are investigated using a DPIV (Digital Particle Image Velocimetry) System. Transverse gust is created by a pitching and plunging flat plate in feathering conditions upstream of the wing in subject, which is a NACA0012 airfoil, and has an aspect ratio of 6. This wing plunges with an amplitude of $h_{amp}/c = 0.25$ at four different frequencies, allowing us to get drag and thrust occurrences in the absence of gust.

METHOD

The experiments are conducted in the large scale, free surface water channel located in the Trisonic Laboratory of Istanbul Technical University, Faculty of Aeronautics and Astronautics. A flat plate as the gust generator and a NACA0012 profile airfoil are mounted in a cantilevered arrangement inside the water channel with an end plate on top to reduce the free surface effects. The gust generator flat plate is mounted from its mid-chord position and the pitching airfoil from its quarter chord position. The Plexiglas flat plate has a chord (c) of 10cm and span (s) of 40cm, the airfoil has a chord (c) of 10cm and span (s) of 30cm. For all cases investigated, the flow speed is 0.1 m/s which corresponds to Reynolds number of 10000. Both mounting beams are connected to pitch motors which are connected to linear tables which allow the plunging motion. The experimental arrangement can be seen in Figure 1.

DPIV (Digital Particle Image Velocimetry) technique is used to record flow fields around and in the near wake of the plunging airfoil and therefore to analyze the vortical structures and the velocity fields. The flow is illuminated by a dual cavity Nd:Yag laser (max. 120mJ/pulse) and the water is seeded with silver coated hollow glass spheres with a mean diameter of 10 μm . The velocity fields are obtained using two 10-bit cameras with 1600 \times 1200 pixels resolution, positioned underneath the water channel. Recorded images are stitched using an in house code and then interrogated using a double frame, cross-correlation technique with a window size of 32 \times 32 pixels and 50% overlapping in each direction.

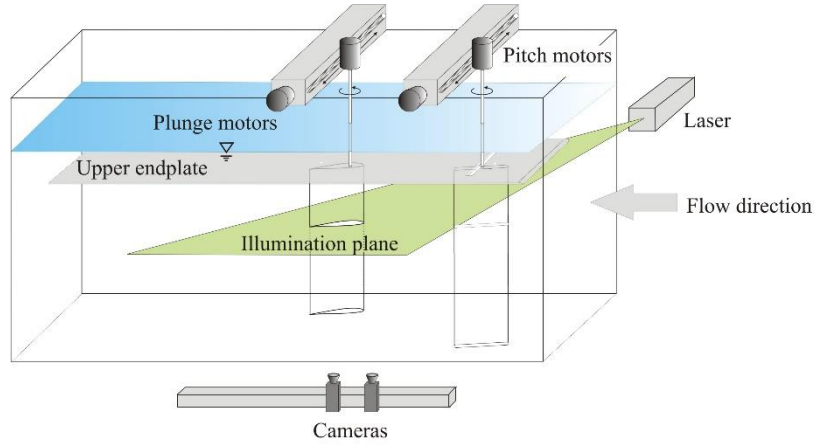


Figure 1: *Experimental setup*

Force and moments acting on the plunging airfoil are measured using a six-component ATI NANO-17 IP68 Force/Torque (F/T) sensor. The sensor is attached to the vertical cantilevered mounting beam of the test model, oriented with its cylindrical z-axis normal to the pitch-plunge plane. The plunge motion of the model, as well as the feathering of the gust generator plate, are accomplished with Kollmorgen/Danaher Motion servo motors which are connected to a computer via ServoSTAR digital servo amplifiers. Motor motion profiles are generated by a signal generator Labview VI (Virtual Instrument) for the given amplitude and frequency. The same VI triggered the PIV system at the beginning of the fifth motion cycle of the airfoil and synchronization is achieved using a National Instruments PCI-6601 timer device. The start of the motion of the wing is also synchronized at four different timings with respect to the motion of the gust generator.

The sinusoidal plunging motion of the airfoil is given as;

$$h(t) = h_{amp} \sin(2\pi ft)$$

where $h(t)$ is the linear plunge motion, transverse to the freestream velocity, h_{amp} is the plunge amplitude and f is the plunging frequency.

In a previous study, periodic vortex gusts are generated in the water channel [Biler et al., 2015]. The spectral analysis of the velocity field in the wake of the oscillating plate were used to characterize the gust. Three different gust types with varying frequencies and amplitudes have been obtained and identified such that all can be considered as spanwise gusts where the streamwise fluctuations are minimized. The plunging NACA0012 airfoil was subjected to these three gust types, as given in Table 1. In addition to the gust cases, No Gust case was also investigated. The test case parameters for the plunging airfoil are plunging frequencies of $f = 0.125\text{Hz}$, 0.25Hz , 0.5Hz and 1.0Hz , h_{amp}/c ratio of 0.25 with gust phase angles of $\phi = 0^\circ$, 90° , 180° and 270° .

Table 1: *Gust parameters*

Gust No	Frequency [Hz]	Amplitude
1	0.5	$0.9 U_\infty$
2	0.25	$0.3 U_\infty$
3	0.25	$0.9 U_\infty$

RESULTS

Quantitative flow visualization with simultaneous direct force/moment measurements are acquired for a NACA0012 airfoil plunging under predefined types of Gust 1, Gust 2 and Gust 3 generated by an upstream gust generator flat plate, in order to determine the gust effects.

Figure 2 shows the lift coefficient C_L for all plunge frequencies at the phase angle of $\phi = 0^\circ$. It can be seen from Figure 2 that the change in lift decreases with the higher plunge frequencies

as compared to the No Gust case, the reason being mostly due to the dominance of the high lift amplitudes generated with the high plunge frequencies.

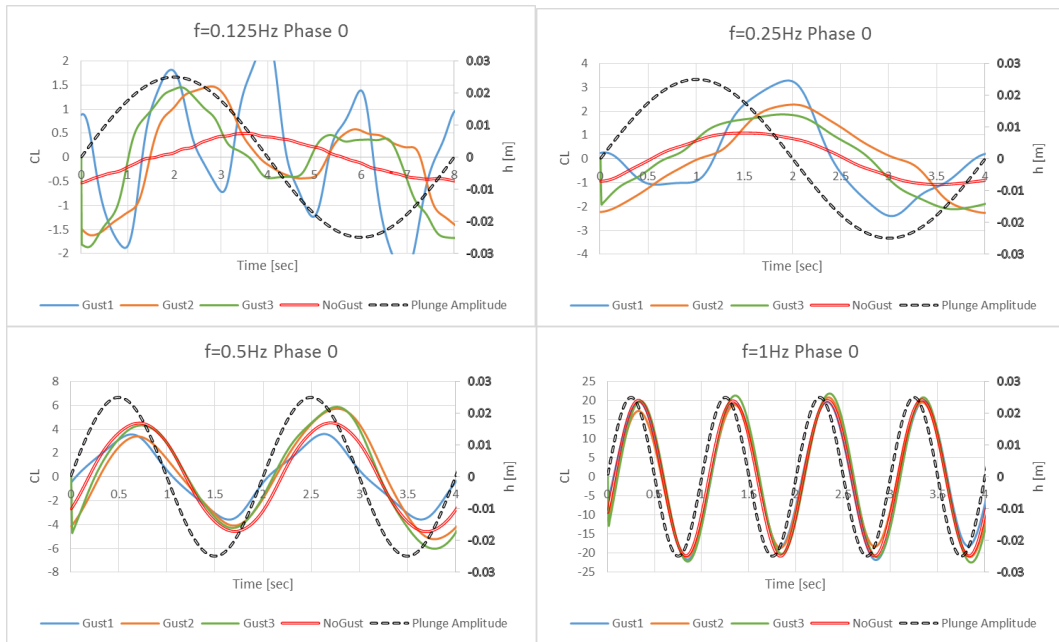


Figure 2: C_L vs time graph at $\phi = 0^\circ$ for all plunge frequencies

In addition, the frequency of gust is more prominent on the amplitude of the lift than the intensity of the gust for the investigated plunge motions. Gust 2 and Gust 3, despite having different intensities, have similar effects on the lift at all investigated plunge frequencies. Both gusts change the amplitude at around the same level but they shift the phase of the lift in different ways. Gust 1, having a higher frequency than Gust 2 and 3, changes the lift amplitude at a higher level.

Airfoil plunging at $f = 0.125\text{Hz}$ demonstrates a greater change in the amplitude from the No Gust case in comparison with the higher plunge frequency cases. The lift values of the cases with gust oscillate around the lift curve of the No Gust case for all phases. The change in the amplitude of the lift is approximately $\Delta C_{L-amp} \approx 2$ for Gust 1 and $\Delta C_{L-amp} \approx 1$ for Gust 2 and 3. Timing of the gust does not change the ΔC_{L-amp} but shifts the phase of the C_L (Figure 3).

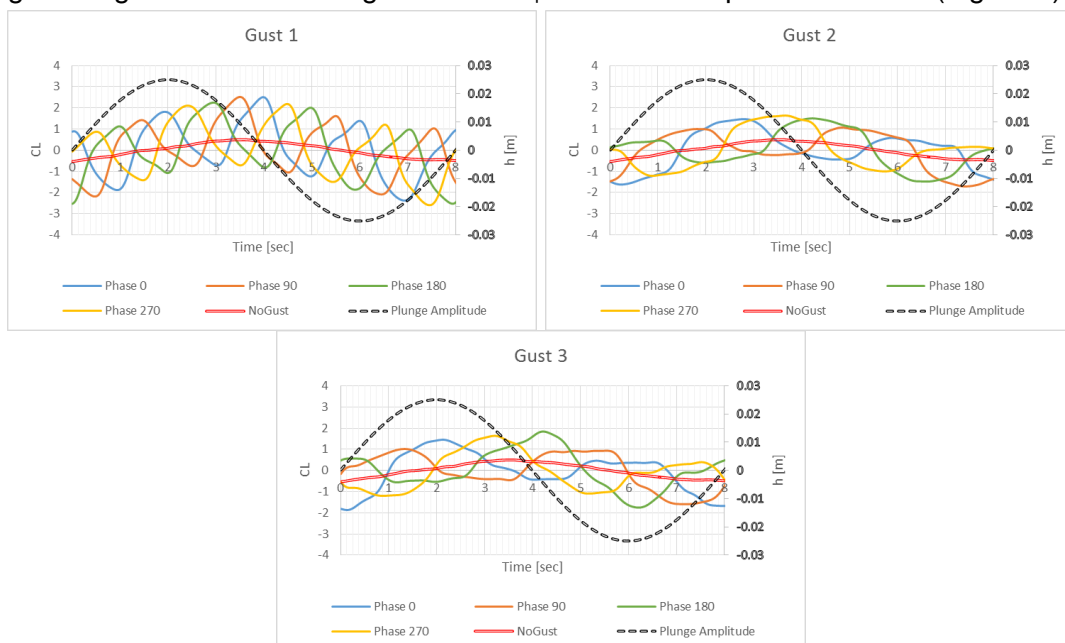


Figure 3: C_L vs time graph for plunge frequency $f = 0.125\text{Hz}$

For the plunge motion at $f = 0.25\text{Hz}$, Figure 4 shows that Gust 1 increases the amplitude of lift around the same values as the plunge motion at $f = 0.125\text{Hz}$ for all phases, approximately at $\Delta C_{L\text{-amp}} \approx 2$. However Gust 2 and 3, being at resonant frequency with the plunge motion, affect the lift differently. Instead of oscillating lift values around the lift curve of the No Gust case, the timing of the Gust 2 and 3 effect both Δ amplitude and the phase of the lift.

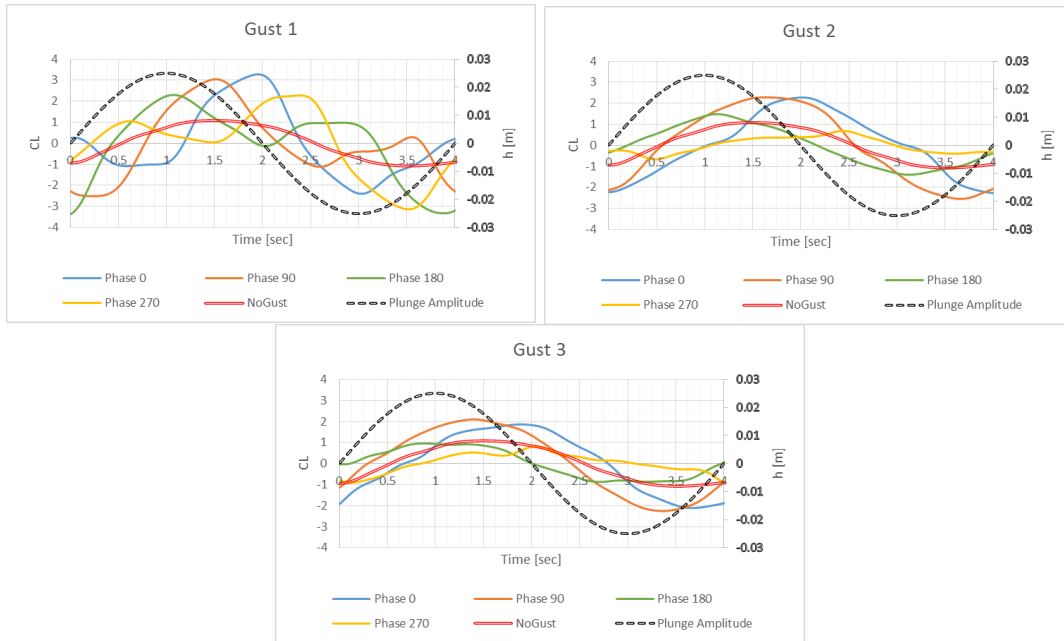


Figure 4: C_L vs time graph for plunge frequency $f = 0.25\text{Hz}$

In a closer look to the resonant cases in Figure 5, the plunge motion at $f = 0.5\text{Hz}$ under Gust 1 shows similar results with the other resonant cases. Timing of the gust affects the $\Delta C_{L\text{-amp}}$ as in $f = 0.25\text{Hz}$ resonant cases. Especially in some phases which have 180° difference show opposite effects. For example in plunge at $f = 0.25\text{Hz}$ under Gust 3, phase 90° increases the amplitude over the No Gust case, whereas phase 270° decreases the amplitude (Figure 6).

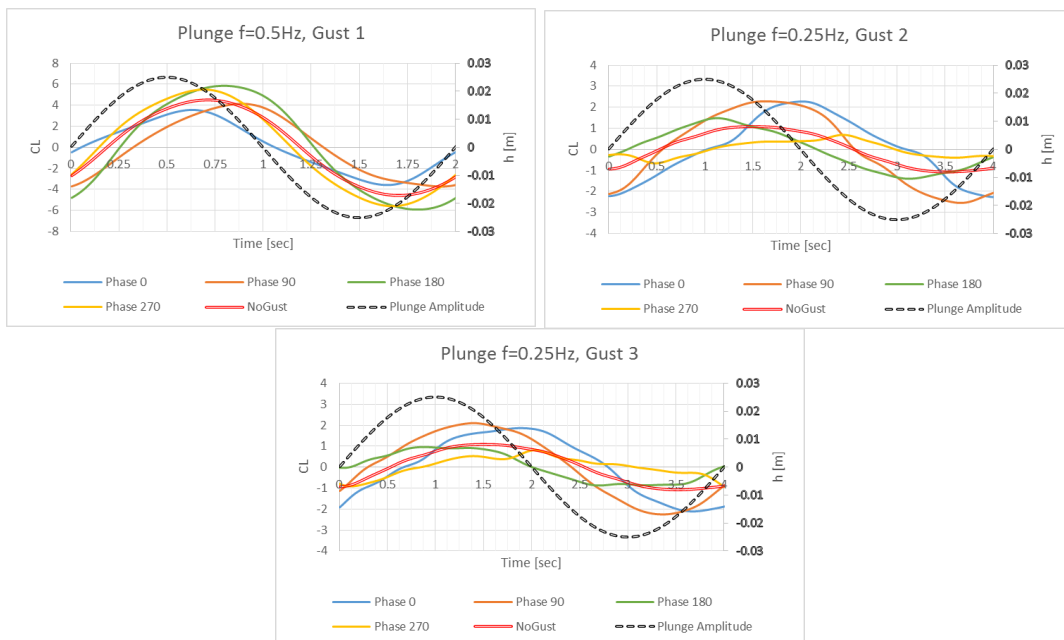


Figure 5: C_L vs time graph for all resonant cases

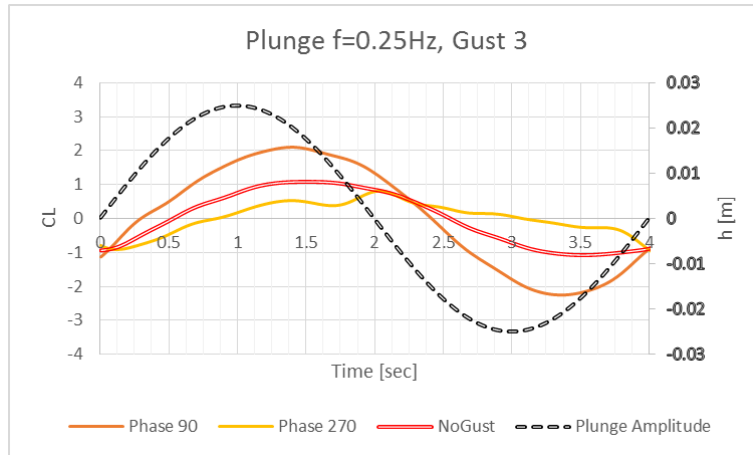


Figure 6: C_L vs time for plunge frequency $f = 0.25\text{Hz}$ under Gust 3 at $\phi = 90^\circ$ and $\phi = 270^\circ$

Figure 7 shows the transverse velocity contours and vorticity contours for the plunge frequency of $f = 0.25\text{Hz}$ under Gust 3 at a phase angle of $\phi = 90^\circ$. The figure shows that the positive transverse velocity caused by the gust increases the lift at the first half of the plunge period; in the second half of the plunge period the lift is decreased by the negative transverse velocity (Figure 7a). Formation of a leading edge vortex (LEV) at $t = 1.5\text{s}$ and $t = 3.5\text{s}$ can be observed in Figure 7b, however the LEV detaches and disperses with the colliding vortices which are generated by the gust. In contrary, at 270° of phase angle, formation of an evident LEV cannot be seen, which lowers the lift amplitude (Figure 8b). Moreover, the arrival of the opposite sign transverse velocities of gust during a plunge period significantly lowers the amplitude of lift (Figure 8a).

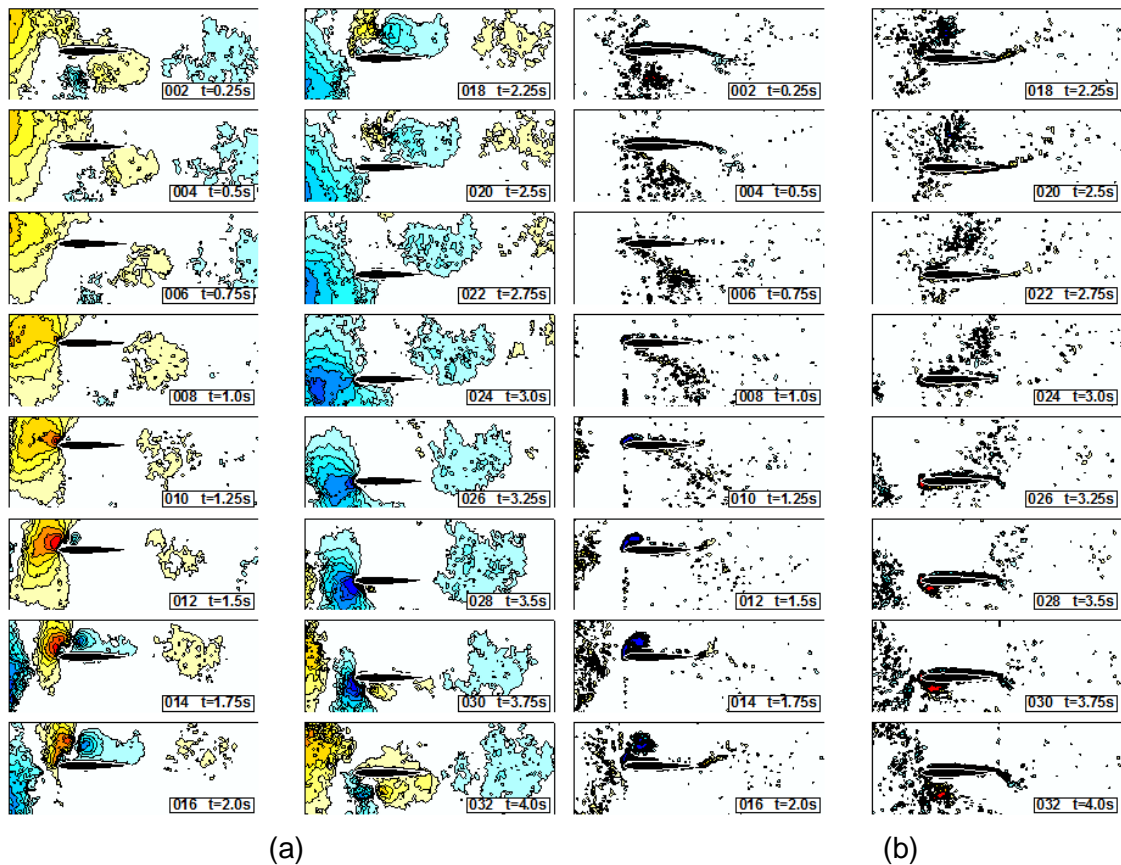


Figure 7: a) Transverse velocity contours, b) Vorticity contours for plunge frequency $f = 0.25\text{Hz}$ under Gust 3 at $\phi = 90^\circ$

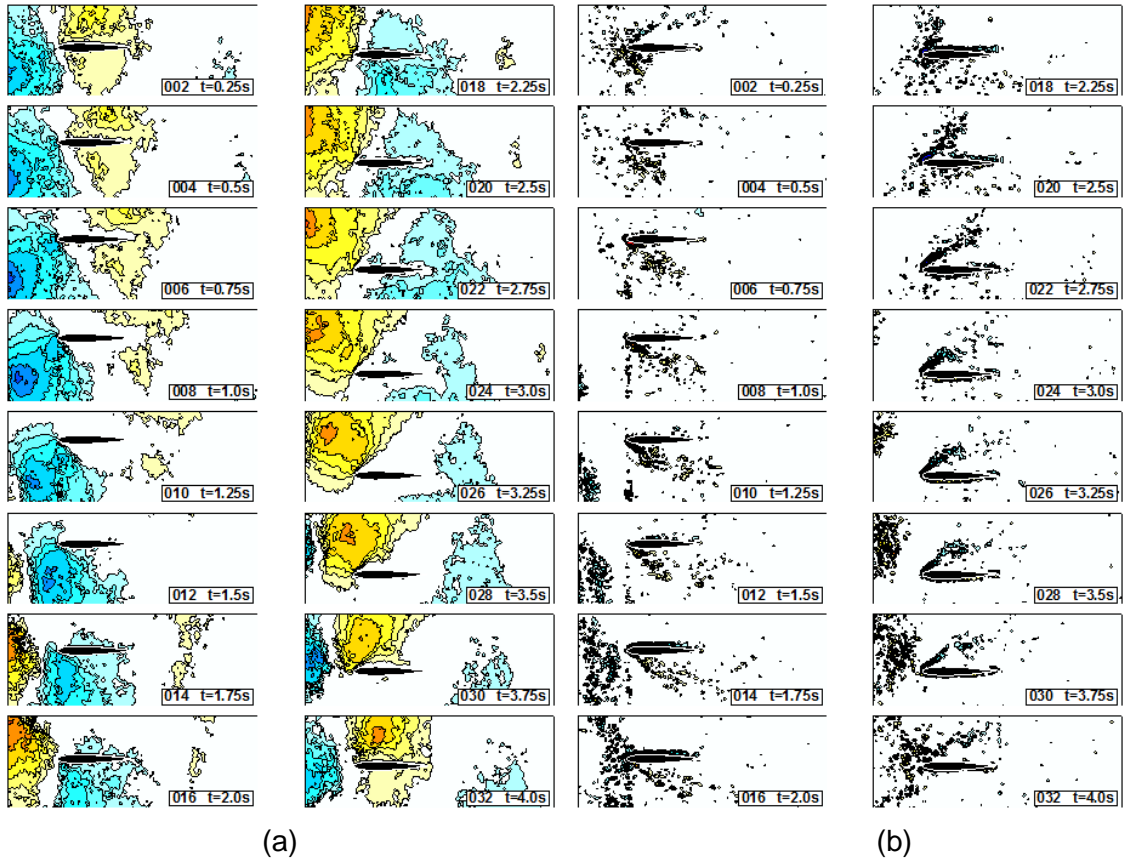


Figure 8: a) Transverse velocity contours, b) Vorticity contours for plunge frequency $f = 0.25\text{Hz}$ under Gust 3 at $\phi = 270^\circ$

In the high plunge frequency case of $f = 1\text{Hz}$, the strong lift force generated by the plunge motion is dominant and the effect caused by the gust is comparatively smaller. There is little or no shift in lift caused by the gust. The very small change in the amplitude of lift can be observed at apices of every two or four period of gust since the plunge frequency doubles or quadruples the frequency of the gust. (Figure 9).

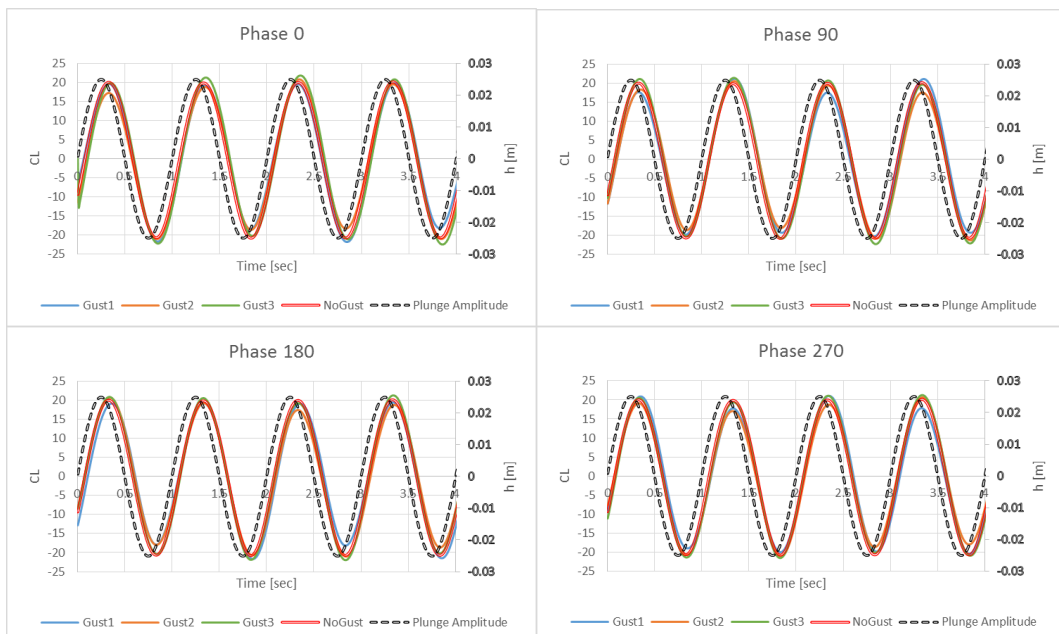


Figure 9: C_L vs time graph for plunge frequency $f = 1\text{Hz}$

CONCLUSIONS

The investigation of the effect of predetermined gusts on a plunging airfoil was conducted by both DPIV and force-moment measurements. The results suggest that the airfoil plunging at low frequencies is more susceptible to the effects of gust on the lift force. With the higher plunge frequencies, the effect of the gust to the total lift force decreases. It was also found that the frequency of gust affects the amplitude of the lift more than the intensity of the gust for the investigated plunge cases. For the cases where the gust frequency is in resonance with the plunge frequency, the timing of the gust changes the amplitude of the lift dramatically.

Acknowledgements

This study is supported by TUBITAK Grant 115M358 (For the Application on UAVs and MAVs, Gust Effect on the Performance of Wings in Motion (Maneuver or Flapping) and Flow Control Attempts).

References

- Biler, H., Zaloglu, B. and Cetiner, O. (2015) Effect of Spanwise Gust on a Wing, 8th Ankara International Aerospace Conference, 10-12 September, METU, Ankara TURKEY.
- Irving J., Smih D., (2013) *Innovative Control Effectors for Manoeuvring Air Vehicles*, NATO AVT-239-RTG-082 Technical Activity Proposal (TAP).
- Jones A., Ol, M.V., (2014a) *Incompressible Aerodynamics of Large Amplitude Gust Encounters for Rigid Bodies*, NATO AVT-ET-154 Technical Activity Proposal (TAP).
- Jones A., Ol, M.V., (2014b) *Incompressible Aerodynamics of Large Gust Encounters for Rigid Bodies*, NATO AVT (Applied Vehicle Technology) - Terms of Reference (ToR) Form.
- Murrow, H. N., Pratt, K. G., Houbolt, J. C. (1989) *NACA/NASA Research Related To Evolution of U.S. Gust Design Criteria*, NASA 89-1373-CP.
- Neumann, J., Mai, H. (2013) *Gust response: Simulation of an aeroelastic experiment by a fluid-structure interaction method*, Journal of Fluids and Structures. 38, 290–302.
- Roadman, J. M., Mohseni, K. (2009) *Gust Characterization and Generation for Wind Tunnel Testing of Micro Aerial Vehicles*, AIAA paper 2009-1290.
- Shao, K., Wu, Z., Yang, C., Chen, L., Lv, B. (2010) *Design of an adaptive gust response alleviation control system: simulations and experiments*, Journal of Aircraft, 47(3), 1022-1029.
- Viswanath, K., Tafti, D.K., (2010) *Effect of frontal gusts on forward flapping flight*, AIAA Journal, 48(9), 2049-2062.
- Watkins, S., Milbank, J., Loxton, B. J., Melbourne, W. H., (2006) *Atmospheric winds and their implications for microair vehicles*, AIAA Journal, 44(11), 2591-2600.